Hierarchical model (Hi-Mod) reduction in non-rectilinear domains

Simona Perotto[1]

1 Introduction and motivations

In [2, 1] we have proposed an approach for the numerical modeling of second-order elliptic problems exhibiting a dominant direction in their behaviour: the solution of interest can be regarded as a main component aligned with the centerline of the domain with the addition of local perturbations along the transverse directions. Reference application is given, e.g., by advection-diffusion-reaction problems in pipes (like drug transport in the circulatory system). The basic idea of the approach is to perform a finite element discretization along the mainstream and a spectral modal approximation for the transverse components. The rationale is that the transverse components are reliably captured by few modes (usually < 10). In addition, the number of modes can locally vary along the centerline to properly fit the transverse behaviour of the solution. Thus we get an actual hierarchy of reduced models: they are essentially locally-enriched 1D models and differ for the level of detail in describing the transverse behaviour of the full problem. For this reason, we defined this approach Hierarchical Model (*Hi-Mod*) reduction.
So far we have essentially applied the Hi-Mod approach to rectilinear domains [1, 2, 4]. This implies significant simplifications in the computation of the reduced model. Nevertheless, domains with a curved centerline are clearly of paramount interest for practical applications. Aim of this paper is to perform a complete development of the Hi-Mod reduction in a generic non-rectilinear domain.

2 The geometrical setting

A Hi-Mod reduction procedure relies upon a specific shape of the computational domain $\Omega \subset \mathrm{I\!R}^d$, with $d = 2,3$. More precisely, we assume Ω to coincide with a d-dimensional *fiber bundle*, where we distinguish a supporting one-dimensional curved domain Ω_{1D} (aligned with the mainstream), and a set of $(d-1)$-dimensional transverse fibers $\gamma \subset \mathrm{I\!R}^{d-1}$ (associated with the transverse components of the solution). Following [1, 2], we map the current domain Ω into a reference domain, $\widehat{\Omega} = \widehat{\Omega}_{1D} \times \widehat{\gamma}_{d-1}$, with $\widehat{\Omega}_{1D}$ a straight line and $\widehat{\gamma}_{d-1}$ a reference (transverse) fiber of the same dimension as γ. For this purpose, we introduce the map $\Psi : \Omega \to \widehat{\Omega}$ and we denote by $\mathbf{z} = (x, \mathbf{y}) \in \Omega$ and $\widehat{\mathbf{z}} = (\widehat{x}, \widehat{\mathbf{y}}) \in \widehat{\Omega}$ a generic point in Ω and the corre-

[1] MOX, Dipartimento di Matematica "F. Brioschi", Politecnico di Milano, Piazza Leonardo da Vinci 32, I-20133 Milano, Italy e-mail: `simona.perotto@polimi.it`

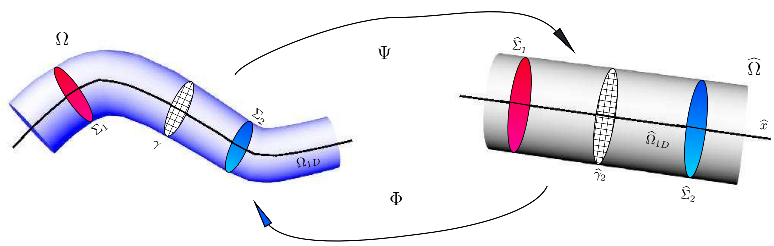

Fig. 1 Sketch of the main geometrical quantites involved in the Hi-Mod procedures ($d = 3$)

sponding point in $\widehat{\Omega}$, respectively so that $\widehat{\mathbf{z}} = \boldsymbol{\Psi}(\mathbf{z}) = (\Psi_1(\mathbf{z}), \Psi_2(\mathbf{z}))$, with $\widehat{x} = \Psi_1(\mathbf{z})$ and $\widehat{\mathbf{y}} = \Psi_2(\mathbf{z})$. Likewise, we introduce the inverse map $\boldsymbol{\Phi} : \widehat{\Omega} \to \Omega$, defined as $\mathbf{z} = \boldsymbol{\Phi}(\widehat{\mathbf{z}}) = (\Phi_1(\widehat{\mathbf{z}}), \Phi_2(\widehat{\mathbf{z}}))$, with $x = \Phi_1(\widehat{\mathbf{z}})$ and $\mathbf{y} = \Phi_2(\widehat{\mathbf{z}})$ (see Fig. 1). Without loss of generality, we assume Ω_{1D} to coincide with the centerline of Ω, and analogously for $\widehat{\Omega}_{1D}$. We assume that both $\boldsymbol{\Psi}$ and $\boldsymbol{\Phi}$ are differentiable with respect to $\mathbf{z}$. Then, we define the Jacobian associated with the map $\boldsymbol{\Psi}$

$$\mathscr{J}(\mathbf{z}) = \frac{\partial \boldsymbol{\Psi}}{\partial \mathbf{z}} = \begin{bmatrix} \dfrac{\partial \Psi_1}{\partial x} & \nabla_{\mathbf{y}} \Psi_1 \\ \dfrac{\partial \Psi_2}{\partial x} & \nabla_{\mathbf{y}} \Psi_2 \end{bmatrix} \in \mathbb{R}^{d \times d}, \tag{1}$$

where $\nabla_{\mathbf{y}}$ is the gradient with respect to $\mathbf{y}$. Notice that the first row in (1) accounts for the centerline deformation and it is not trivially the first row of the identity matrix as in the rectilinear case ([2]).

3 The Hi-Mod reduction procedure

Let us first introduce the model we aim at reducing, i.e., the so-called *full problem*. In particular, we consider directly the weak formulation, given by

$$\text{find } u \in V \quad : \quad a(u,v) = F(v) \quad \forall v \in V, \tag{2}$$

with V a Hilbert space, $a(\cdot,\cdot) : V \times V \to \mathbb{R}$ a continuous and coercive bilinear form and $F(\cdot) : V \to \mathbb{R}$ a continuous linear functional. Since we deal with second-order elliptic problems, we have $V \subseteq H^1(\Omega)$.

The Hi-Mod reduction strongly relies upon the fiber structure of Ω. The idea is to tackle the dominant and transverse components of the solution in different ways. In particular, with reference to $\widehat{\Omega}$, we introduce a one-dimensional space $V_{\widehat{\Omega}_{1D}}$ of functions compatible with the boundary conditions assigned along the extremal faces of Ω, and a modal basis $\{\varphi_k\}_{k \in \mathbb{N}^+}$ of functions orthonormal with respect to the L^2-scalar product on $\widehat{\gamma}_{d-1}$ and taking into account the boundary conditions imposed on the lateral faces of Ω. A suitable combination of the space $V_{\widehat{\Omega}_{1D}}$ with the modal basis allows us to introduce a so-called *hierarchically reduced model*. In particular, in the following, we focus on two possible Hi-Mod reduction procedures proposed in [1, 2] and here generalized to the non-rectilinear case.

3.1 Uniform Hi-Mod reduction

The reduced space V_m characterizing a uniform Hi-Mod reduction essentially coincides with the set of the linear combinations of the modal functions whose coefficients belong to the one-dimensional space $V_{\widehat{\Omega}_{1D}}$, i.e.,

$$V_m = \Big\{ v_m(\mathbf{z}) = \sum_{k=1}^{m} v_k(\Psi_1(\mathbf{z}))\varphi_k(\Psi_2(\mathbf{z})), \text{ with } v_k \in V_{\widehat{\Omega}_{1D}} \Big\}. \tag{3}$$

The map Ψ plays a crucial role since all the functions involved are defined on the reference framework. Space V_m establishes an actual *hierarchy* of reduced models marked by the modal index m, i.e., by the different level of detail in describing the transverse behaviour of the full solution. The uniform Hi-Mod reduced formulation for (2) reads: given a modal index $m \in \mathbb{N}^+$, find $u_m \in V_m$, such that

$$a(u_m, v_m) = F(v_m) \quad \forall v_m \in V_m. \tag{4}$$

To guarantee the well-posedness and the convergence of u_m to u, we introduce a conformity ($V_m \subset V, \forall m \in \mathbb{N}^+$) and a spectral approximability ($\lim_{m\to+\infty}(\inf_{v_m\in V_m} \|v - v_m\|_V) = 0, \forall v \in V$) assumptions on V_m ([1, 2]).

Let us detail now the uniform Hi-Mod reduction procedure on a specific differential problem. In particular, we select the full model (2) as a standard linear scalar advection-diffusion-reaction (ADR) problem completed with full homogeneous Dirichlet boundary conditions, so that $V = H_0^1(\Omega)$,

$$a(u,v) = \int_\Omega \mu \nabla u \cdot \nabla v \, d\Omega + \int_\Omega \big(\mathbf{b}\cdot\nabla u + \sigma u\big) v \, d\Omega, \qquad F(v) = \int_\Omega f v \, d\Omega, \tag{5}$$

and where the following choices are made for the problem data to ensure the well-posedness of the weak form (2): $f \in L^2(\Omega)$, $\mu \in L^\infty(\Omega)$, with $\mu \geq \mu_0 > 0$ a.e. in Ω, $\sigma \in L^\infty(\Omega)$, $\mathbf{b} = (b_1, \mathbf{b}_2)^T \in L^\infty(\Omega) \times [L^\infty(\Omega)]^{d-1}$, with $\nabla \cdot \mathbf{b} \in L^\infty(\Omega)$ and such that $-\frac{1}{2}\nabla\cdot\mathbf{b} + \sigma \geq 0$ a.e. in Ω.
Now we consider the reduced model (4); we replace u_m with the corresponding modal representation $u_m(\mathbf{z}) = \sum_{j=1}^m u_j(\Psi_1(\mathbf{z}))\varphi_j(\Psi_2(\mathbf{z}))$ and v_m with the product $\vartheta(\Psi_1(\mathbf{z}))\varphi_k(\Psi_2(\mathbf{z}))$, where $\vartheta, u_j \in V_{\widehat{\Omega}_{1D}} = H_0^1(\widehat{\Omega}_{1D})$ for $j = 1, \ldots, m$, to get

$$\sum_{j=1}^{m} \Big[\int_\Omega \mu(\mathbf{z}) \nabla\big(u_j(\Psi_1(\mathbf{z}))\, \varphi_j(\Psi_2(\mathbf{z}))\big) \cdot \nabla\big(\vartheta(\Psi_1(\mathbf{z}))\, \varphi_k(\Psi_2(\mathbf{z}))\big)\, d\Omega \tag{6}$$

$$+\int_{\Omega} \mathbf{b}(\mathbf{z})\cdot\nabla\big(u_j(\Psi_1(\mathbf{z}))\,\varphi_j(\Psi_2(\mathbf{z}))\big)\,\vartheta(\Psi_1(\mathbf{z}))\,\varphi_k(\Psi_2(\mathbf{z}))\,d\Omega$$
$$+\int_{\Omega} \sigma(\mathbf{z})u_j(\Psi_1(\mathbf{z}))\,\varphi_j(\Psi_2(\mathbf{z}))\,\vartheta(\Psi_1(\mathbf{z}))\,\varphi_k(\Psi_2(\mathbf{z}))\,d\Omega\Big]$$
$$=\int_{\Omega} f(\mathbf{z})\,\vartheta(\Psi_1(\mathbf{z}))\,\varphi_k(\Psi_2(\mathbf{z}))\,d\Omega,$$

where ∇ denotes the gradient with respect to $\mathbf{z}$. The actual unknowns of the Hi-Mod reduced formulation (4) are the modal coefficients $u_j \in V_{\widehat{\Omega}_{1D}}$. We expand separately the four integrals, by exploiting the gradient expansion

$$\nabla(w(\Psi_1(\mathbf{z}))\varphi_s(\Psi_2(\mathbf{z}))) =$$
$$w'(\Psi_1(\mathbf{z}))\varphi_s(\Psi_2(\mathbf{z}))\begin{bmatrix}\dfrac{\partial\Psi_1(\mathbf{z})}{\partial x}\\ \nabla_{\mathbf{y}}\Psi_1(\mathbf{z})\end{bmatrix} + w(\Psi_1(\mathbf{z}))\varphi_s'(\Psi_2(\mathbf{z}))\begin{bmatrix}\dfrac{\partial\Psi_2(\mathbf{z})}{\partial x}\\ \nabla_{\mathbf{y}}\Psi_2(\mathbf{z})\end{bmatrix},$$

where $w'(\Psi_1(\mathbf{z})) = dw/d\widehat{x}|_{\widehat{x}=\Psi_1(\mathbf{z})}$, $\varphi_s'(\Psi_2(\mathbf{z})) = d\varphi_s/d\widehat{\mathbf{y}}|_{\widehat{\mathbf{y}}=\Psi_2(\mathbf{z})}$ and with $w \in V_{\widehat{\Omega}_{1D}}$. The idea is to rewrite each term on the reference domain by properly exploiting the maps Ψ, Φ. Let us first consider the diffusive contribution in (6):

$$\begin{aligned}
&\int_{\widehat{\Omega}} \mu(\Phi(\widehat{\mathbf{z}}))\Big\{\Big[\Big(\frac{\partial\Psi_1(\Phi(\widehat{\mathbf{z}}))}{\partial x}\Big)^2 + \big(\nabla_{\mathbf{y}}\Psi_1(\Phi(\widehat{\mathbf{z}}))\big)^2\Big]\varphi_j(\widehat{\mathbf{y}})\varphi_k(\widehat{\mathbf{y}})u_j'(\widehat{x})\vartheta'(\widehat{x})\\
&+\Big[\frac{\partial\Psi_1(\Phi(\widehat{\mathbf{z}}))}{\partial x}\frac{\partial\Psi_2(\Phi(\widehat{\mathbf{z}}))}{\partial x} + \nabla_{\mathbf{y}}\Psi_1(\Phi(\widehat{\mathbf{z}}))\nabla_{\mathbf{y}}\Psi_2(\Phi(\widehat{\mathbf{z}}))\Big]\\
&\quad\big[\varphi_j(\widehat{\mathbf{y}})\varphi_k'(\widehat{\mathbf{y}})u_j'(\widehat{x})\vartheta(\widehat{x}) + \varphi_j'(\widehat{\mathbf{y}})\varphi_k(\widehat{\mathbf{y}})u_j(\widehat{x})\vartheta'(\widehat{x})\big]\\
&+\Big[\Big(\frac{\partial\Psi_2(\Phi(\widehat{\mathbf{z}}))}{\partial x}\Big)^2 + \big(\nabla_{\mathbf{y}}\Psi_2(\Phi(\widehat{\mathbf{z}}))\big)^2\Big]\varphi_j'(\widehat{\mathbf{y}})\varphi_k'(\widehat{\mathbf{y}})u_j(\widehat{x})\vartheta(\widehat{x})\Big\}\,|\mathscr{I}^{-1}(\Phi(\widehat{\mathbf{z}}))|\,d\widehat{\Omega},
\end{aligned}\tag{7}$$

with $\mathscr{I}$ the Jacobian defined in (1). The convective term is changed into

$$\begin{aligned}
&\int_{\widehat{\Omega}}\Big\{\Big[b_1(\Phi(\widehat{\mathbf{z}}))\frac{\partial\Psi_1(\Phi(\widehat{\mathbf{z}}))}{\partial x} + \mathbf{b}_2(\Phi(\widehat{\mathbf{z}}))\nabla_{\mathbf{y}}\Psi_1(\Phi(\widehat{\mathbf{z}}))\Big]\varphi_j(\widehat{\mathbf{y}})\varphi_k(\widehat{\mathbf{y}})u_j'(\widehat{x})\vartheta(\widehat{x})\\
&\quad\Big[b_1(\Phi(\widehat{\mathbf{z}}))\frac{\partial\Psi_2(\Phi(\widehat{\mathbf{z}}))}{\partial x} + \mathbf{b}_2(\Phi(\widehat{\mathbf{z}}))\nabla_{\mathbf{y}}\Psi_2(\Phi(\widehat{\mathbf{z}}))\Big]\varphi_j'(\widehat{\mathbf{y}})\varphi_k(\widehat{\mathbf{y}})u_j(\widehat{x})\vartheta(\widehat{x})\Big\}\\
&\quad|\mathscr{I}^{-1}(\Phi(\widehat{\mathbf{z}}))|\,d\widehat{\Omega},
\end{aligned}\tag{8}$$

while, for the reactive term, we have

$$\int_{\widehat{\Omega}} \sigma(\Phi(\widehat{\mathbf{z}}))\varphi_j(\widehat{\mathbf{y}})\varphi_k(\widehat{\mathbf{y}})u_j(\widehat{x})\vartheta(\widehat{x})|\mathscr{I}^{-1}(\Phi(\widehat{\mathbf{z}}))|\,d\widehat{\Omega}. \tag{9}$$

Finally, for the source term in (6), we simply obtain

$$\int_{\widehat{\Omega}} f(\Phi(\widehat{\mathbf{z}}))\varphi_k(\widehat{\mathbf{y}})\vartheta(\widehat{x})|\mathscr{I}^{-1}(\Phi(\widehat{\mathbf{z}}))|\,d\widehat{\Omega}. \tag{10}$$

From (7) we notice that the treatment of the diffusive term generates advective and reactive contributions in the reduced setting. Similarly, the reduced convection term (8) features also a reactive contribution. A straightforward combination of (7)-(10) leads to the following Hi-Mod reduced formulation for the ADR problem defined in (5): find $u_j \in V_{\widehat{\Omega}_{1D}}$ with $j = 1, \ldots, m$, such that, for any $\vartheta \in V_{\widehat{\Omega}_{1D}}$ and $k = 1, \ldots, m$,

$$\sum_{j=1}^{m} \Big\{ \int_{\widehat{\Omega}_{1D}} \Big[\widehat{r}_{kj}^{1,1}(\widehat{x})\, u_j'(\widehat{x})\, \vartheta'(\widehat{x}) + \widehat{r}_{kj}^{1,0}(\widehat{x})\, u_j'(\widehat{x})\, \vartheta(\widehat{x}) + \widehat{r}_{kj}^{0,1}(\widehat{x})\, u_j(\widehat{x})\, \vartheta'(\widehat{x}) \tag{11}$$
$$+ \ \widehat{r}_{kj}^{0,0}(\widehat{x})\, u_j(\widehat{x})\, \vartheta(\widehat{x}) \Big] d\widehat{x} \Big\} = \int_{\widehat{\Omega}_{1D}} \Big[\int_{\widehat{\gamma}_{d-1}} f(\Phi(\widehat{\mathbf{z}}))\varphi_k(\widehat{\mathbf{y}}) |\mathscr{J}^{-1}(\Phi(\widehat{\mathbf{z}}))|\, d\widehat{\mathbf{y}} \Big] \vartheta(\widehat{x})\, d\widehat{x},$$

where

$$\widehat{r}_{kj}^{s,t}(\widehat{x}) = \int_{\widehat{\gamma}_{d-1}} r_{kj}^{s,t}(\widehat{x}, \widehat{\mathbf{y}})\, |\mathscr{J}^{-1}(\Phi(\widehat{\mathbf{z}}))|\, d\widehat{\mathbf{y}}, \quad s,t = 0,1, \quad k = 1, \ldots, m, \tag{12}$$

with

$$\begin{aligned} r_{kj}^{1,1}(\widehat{\mathbf{z}}) &= \mu(\Phi(\widehat{\mathbf{z}}))\, \alpha_1(\widehat{\mathbf{z}})\, \varphi_j(\widehat{\mathbf{y}})\varphi_k(\widehat{\mathbf{y}}), \quad r_{kj}^{0,1}(\widehat{\mathbf{z}}) = \mu(\Phi(\widehat{\mathbf{z}}))\, \delta(\widehat{\mathbf{z}})\, \varphi_j'(\widehat{\mathbf{y}})\varphi_k(\widehat{\mathbf{y}}), \\ r_{kj}^{1,0}(\widehat{\mathbf{z}}) &= \mu(\Phi(\widehat{\mathbf{z}}))\, \delta(\widehat{\mathbf{z}})\, \varphi_j(\widehat{\mathbf{y}})\varphi_k'(\widehat{\mathbf{y}}) + \beta_1(\widehat{\mathbf{z}})\, \varphi_j(\widehat{\mathbf{y}})\varphi_k(\widehat{\mathbf{y}}), \\ r_{kj}^{0,0}(\widehat{\mathbf{z}}) &= \mu(\Phi(\widehat{\mathbf{z}}))\, \alpha_2(\widehat{\mathbf{z}})\varphi_j'(\widehat{\mathbf{y}})\varphi_k'(\widehat{\mathbf{y}}) + \beta_2(\widehat{\mathbf{z}})\, \varphi_j'(\widehat{\mathbf{y}})\varphi_k(\widehat{\mathbf{y}}) + \sigma(\Phi(\widehat{\mathbf{z}}))\, \varphi_j(\widehat{\mathbf{y}})\varphi_k(\widehat{\mathbf{y}}), \end{aligned} \tag{13}$$

and

$$\begin{aligned} \alpha_i(\widehat{\mathbf{z}}) &= \Big(\frac{\partial \Psi_i(\Phi(\widehat{\mathbf{z}}))}{\partial x} \Big)^2 + \big(\nabla_{\mathbf{y}} \Psi_i(\Phi(\widehat{\mathbf{z}})) \big)^2 \quad i = 1,2, \\ \beta_i(\widehat{\mathbf{z}}) &= b_1(\Phi(\widehat{\mathbf{z}})) \frac{\partial \Psi_i(\Phi(\widehat{\mathbf{z}}))}{\partial x} + \mathbf{b}_2(\Phi(\widehat{\mathbf{z}})) \cdot \nabla_{\mathbf{y}} \Psi_i(\Phi(\widehat{\mathbf{z}})) \quad i = 1,2, \\ \delta(\widehat{\mathbf{z}}) &= \frac{\partial \Psi_1(\Phi(\widehat{\mathbf{z}}))}{\partial x} \frac{\partial \Psi_2(\Phi(\widehat{\mathbf{z}}))}{\partial x} + \nabla_{\mathbf{y}} \Psi_1(\Phi(\widehat{\mathbf{z}})) \cdot \nabla_{\mathbf{y}} \Psi_2(\Phi(\widehat{\mathbf{z}})). \end{aligned} \tag{14}$$

In the reduced model (11) the dependence of the solution on the dominant and on the transverse directions is split. The Hi-Mod reduction procedure yields a *special one-dimensional model* associated with the main curved stream, whose coefficients, $\widehat{r}_{kj}^{s,t}$, are properly enriched to include the effects of the transverse components. In particular, the coefficients in (13) reduce to the ones in [1] for rectilinear domains, where $\partial \Psi_1 / \partial x = 1$ and $\nabla_{\mathbf{y}} \Psi_1 = 0$. From a computational viewpoint, the solution to (11) requires solving a system of m coupled one-dimensional problems instead of a full d-dimensional problem. Following [1, 2], we discretize these 1D problems by introducing a finite element discretization along $\widehat{\Omega}_{1D}$, while preserving the modal expansion in correspondence with the transverse directions. We are led to solve a linear system with an $m \times m$ block matrix, where each block is an $N_h \times N_h$ matrix with the sparsity pattern of the selected finite element space X_h, with $\dim(X_h) = N_h$. An appropriate choice of the modal index m in (3) is certainly a critical issue of the uniform Hi-Mod reduction. In [2] a "trial and error" approach is suggested:

we move from the computationally cheapest choice $m = 1$ and then we gradually increase such a value until the addition of the successive modal function does not significantly improve the accuracy of the reduced solution. This strategy may be sometimes speeded up, e.g., when a partial physical knowledge of the phenomenon at hand is available, so that the initial guess can be properly calibrated.

3.2 Piecewise Hi-Mod reduction

The uniform approach may become really uneffective when the meaningful transverse components of the solution are strongly localized: a large number of modal functions is employed on the whole Ω, even though it would be strictly necessary only where significant transverse components are present. This justifies the proposal of a new formulation, where a different number of modes is employed in different parts of Ω: many modes where the transverse components are important, few modes where these are less significant. The modal index m becomes therefore a piecewise constant vector: this justifies the name of this approach. In more detail, let us assume to locate s subdomains Ω_i in Ω such that $\overline{\Omega} = \cup_{i=1}^{s} \overline{\Omega}_i$, with $\Sigma_i = \overline{\Omega}_i \cap \overline{\Omega}_{i+1}$ the interface between Ω_i and Ω_{i+1}, and let $\{\widehat{\Omega}_i\}_{i=1}^{s}$ be the corresponding partition on $\widehat{\Omega}$, with $\widehat{\Sigma}_i = \Psi(\Sigma_i) = \overline{\widehat{\Omega}}_i \cap \overline{\widehat{\Omega}}_{i+1}$ (see Fig. 1). In particular, we employ m_i modal functions on Ω_i, for $i = 1, \ldots, s$. Following [3], the piecewise Hi-Mod reduced formulation for (2) reads: given a modal multi-index $\mathbf{m} = \{m_i\}_{i=1}^{s} \in [\mathbb{N}^+]^s$, find $u_{\mathbf{m}} \in V_{\mathbf{m}}^{b}$, such that

$$a_{\Omega}(u_{\mathbf{m}}, v_{\mathbf{m}}) = F_{\Omega}(v_{\mathbf{m}}) \quad \forall v_{\mathbf{m}} \in V_{\mathbf{m}}^{b}, \tag{15}$$

where $a_{\Omega}(u_{\mathbf{m}}, v_{\mathbf{m}}) = \sum_{i=1}^{s} a_i(u_{\mathbf{m}}|_{\Omega_i}, v_{\mathbf{m}}|_{\Omega_i})$, $F_{\Omega}(v_{\mathbf{m}}) = \sum_{i=1}^{s} F_i(v_{\mathbf{m}}|_{\Omega_i})$ with $a_i(\cdot,\cdot)$ and $\mathscr{F}_i(\cdot)$ the restriction to Ω_i of the bilinear and of the linear form in (2), respectively. The reduced space in (15) is a subset of the broken Sobolev space $H^1(\Omega, \mathscr{T}_{\Omega})$ associated with the partition $\mathscr{T}_{\Omega} = \{\Omega_i\}_{i=1}^{s}$, and it is defined by

$$\begin{aligned} V_{\mathbf{m}}^{b} = \Big\{ & v_{\mathbf{m}} \in L^2(\Omega) \,:\, v_{\mathbf{m}}|_{\Omega_i}(\mathbf{z}) = \sum_{k=1}^{m_i} v_k^i(\Psi_1(\mathbf{z}))\, \varphi_k(\Psi_2(\mathbf{z})) \in H^1(\Omega_i) \\ & \forall i = 1, \ldots, s, \text{ with } v_k^i \in H^1(\widehat{\Omega}_{1D,i}) \text{ and s.t., } \forall k = 1, \ldots, m_{\perp}^{j} \text{ with } j = 1, \ldots, s-1, \\ & \int_{\widehat{\gamma}_{d-1}} \big[v_{\mathbf{m}}|_{\Omega_{j+1}}(\Phi(\widehat{\Sigma}_j)) - v_{\mathbf{m}}|_{\Omega_j}(\Phi(\widehat{\Sigma}_j)) \big]\, \varphi_k(\widehat{\mathbf{y}})\, d\widehat{\mathbf{y}} = 0 \Big\}, \end{aligned}$$

with $m_{\perp}^{j} = \min(m_j, m_{j+1})$ and $\widehat{\Omega}_{1D,i} = \widehat{\Omega}_{1D} \cap \widehat{\Omega}_i$. The integral condition weakly enforces the continuity of the solution in correspondence with the minimum number of modes employed on the whole Ω. This does not guarantee *a priori* the conformity of the reduced solution $u_{\mathbf{m}}$ (see section 4.2.2 in [2] for more details). According to [3], we resort to a relaxed iterative substructuring Dirichlet/Neumann method to impose the weak continuity at the interfaces. From a computational viewpoint, at each iteration of the Dirichlet/Neumann scheme, we apply a uniform Hi-Mod reduction on each subdomain Ω_i, i.e., we solve s systems of coupled 1D problems which are

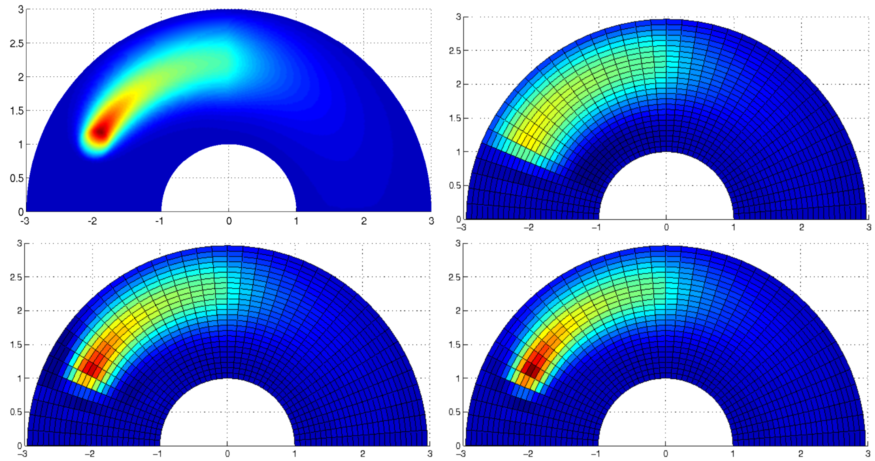

Fig. 2 Full solution and uniform Hi-Mod reduced solutions u_3, u_5, u_7 (top-bottom, left-right)

suitably approximated via a finite element discretization along $\widehat{\Omega}_{1D}$, analogously to the uniform case. The choice of the modal multi-index $\mathbf{m}$ in (15) is hereafter based on an *a priori* approach, driven by some knowledge of the solution u. The generalization of the approach proposed in [3] for rectilinear domains, where an *a posteriori* modeling error estimator drives the automatic selection of both the Ω_i's and $\mathbf{m}$ is a possible follow up of this work.

4 Numerical results

We numerically assess the two proposed Hi-Mod reduction procedures in a two-dimensional setting. In particular, we use affine finite elements to discretize the problem along $\widehat{\Omega}_{1D}$, while employing sinusoidal functions to model the transverse components. We evaluate the integrals of the sine functions via Gaussian quadrature formulas, with, at least, four quadrature nodes per wavelenght. Of course, different choices are possible for the modal basis (Legendre polynomials, wavelets, suitable eigenfunctions).

We reduce the ADR problem defined in (5) on the annular region Ω between the two concentric circles $x^2+y^2=1$ and $x^2+y^2=9$. We select $\mu=1$, the circular clockwise advective field $\mathbf{b}=\big(30\sin(\text{atan2}(y,x)),-30\cos(\text{atan2}(y,x))\big)^T$, with $-\pi\leq\text{atan2}(y,x)\leq\pi$, $\sigma=30\chi_+$ with $\chi_+=\{(x,y)\in\Omega : x>0\}$, and the source term $f=1000\chi_D$ localized in the small circular region $D=\{(x,y):(x+2)^2+(y-1)^2<0.05\}$. Finally, full homogeneous Dirichlet boundary conditions complete the problem. The choice of the data identifies a full solution characterized by a peak in D; it is convected by the field $\mathbf{b}$ and damped by the reaction (see Fig. 2, top-left).

Figure 2 gathers the reduced solutions provided by the uniform Hi-Mod reduction

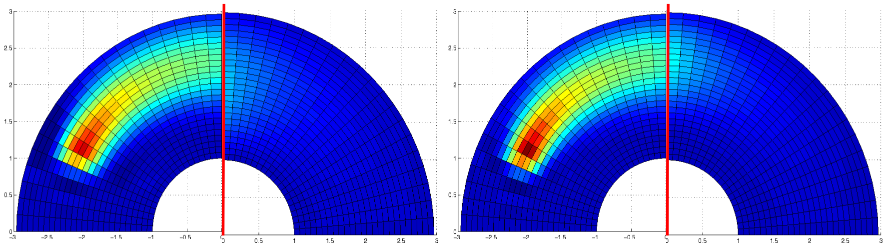

Fig. 3 Piecewise Hi-Mod reduced solutions $u_{\{5,1\}}$ (left) and $u_{\{7,3\}}$ (right)

for different choices of the modal index m and when a uniform finite element discretization of size $h = \pi/40$ is employed on $\widehat{\Omega}_{1D}$. Solution u_3 clearly fails in detecting the peak in D. At least seven modal functions are demanded to get a reliable reduced model: the peak of u is well captured for this choice, while the successive modes essentially do not improve the accuracy of u_m.

The most significant localization of the transverse components in the left part of Ω suggests us employing a higher number of modes in this part of the domain, according to a piecewise Hi-Mod reduction. We split Ω into two subdomains via the interface $\Sigma_1 = \{0\} \times (1,3)$; then we make two different choices for the modal multi-index, $\mathbf{m} = \{5,1\}$ and $\mathbf{m} = \{7,3\}$, while preserving the finite element partition of the uniform approach. Concerning the domain decomposition algorithm, we set the convergence tolerance for the relative error to 10^{-3} and the relaxation parameter to 0.5. Moreover, to guarantee the well-posedness of the ADR subproblems, we assign the Dirichlet and the Neumann condition on the right- and on the left-hand side of Σ_1, respectively. The algorithm converges after ten iterations for both choices of $\mathbf{m}$. Figure 3 shows the reduced solutions $u_{\{5,1\}}$ (left) and $u_{\{7,3\}}$ (right) at the last iteration. As expected, $u_{\{7,3\}}$ provides a better approximation of the full solution; in particular, by comparing the color maps, we can state that $u_{\{7,3\}}$ essentially coincides with u_7 in Fig. 2, bottom-right. Finally, according to [2], both $u_{\{5,1\}}$ and $u_{\{7,3\}}$ are H^1-conforming approximations: the model discontinuity across Σ_1 is therefore consequence of the truncation of the iterative domain decomposition algorithm.

References

1. Ern, A., Perotto, S., Veneziani, A.: Hierarchical model reduction for advection-diffusion-reaction problems. In: K. Kunisch, G. Of, O. Steinbach (eds.) Numerical Mathematics and Advanced Applications, pp. 703–710. Springer–Verlag (2008)
2. Perotto, S., Ern, A., Veneziani, A.: Hierarchical local model reduction for elliptic problems: a domain decomposition approach. Multiscale Modeling & Simulation **8**(4), 1102–1127 (2010)
3. Perotto, S., Ern, A., Veneziani, A.: Coupled adaptive model reduction and discretization for elliptic problems: a hierarchical approach. In preparation (2013)
4. Perotto, S., Zilio, A.: Hierarchical model reduction: three different approaches. In: A. Cangiani, R. Davidchack, E. Georgoulis, A. Gorban, J. Levesley, M. Tretyakov (eds.) Numerical Mathematics and Advanced Applications. Springer–Verlag (2013)